

Quasiparticle interference scattering of spin-polarized Shockley-like surface state electrons: Ni(111)Andreas Krönlein,¹ Jeannette Kemmer,¹ Pin-Jui Hsu,^{1,*} and Matthias Bode^{1,2}¹*Physikalisches Institut, Universität Würzburg, Am Hubland, 97074 Würzburg, Germany*²*Wilhelm Conrad Röntgen-Center for Complex Material Systems (RCCM), Universität Würzburg, Am Hubland, 97074 Würzburg, Germany*

(Received 3 February 2014; revised manuscript received 20 March 2014; published 8 April 2014)

We report on a detailed quasiparticle interference (QPI) scattering study of the Ni(111) surface by low-temperature scanning tunneling spectroscopy (LT-STs). While conventional constant-separation STs shows two broad features, which are interpreted as the Λ_3 bulk band and sp -like Shockley-type surface state (sp -SS), energy-dependent Fourier-transformed QPI maps reveal the band dispersion of the underlying surface electronic features. We find two electronlike branches in the sp -SS dispersion, which are interpreted as the exchange-split minority and majority spin part. The exchange splitting is determined to $\Delta E_{\text{ex}} = 100 \pm 8$ meV. In addition, a holelike d -derived surface resonance is found. Band onsets and effective electron masses are determined by fitting the band dispersion with a parabola at small k values. Hybridization effects with bulk electronic states are observed towards larger k values. Prominent quantum confinement phenomena of the sp -SS are observed in STs data obtained within vacancy islands. The results can be interpreted within a one-dimensional quantum-well model.

DOI: [10.1103/PhysRevB.89.155413](https://doi.org/10.1103/PhysRevB.89.155413)

PACS number(s): 68.37.Ef, 73.20.At, 75.30.Et, 79.60.Bm

I. INTRODUCTION

As a consequence of the particle-wave duality [1], the elastic scattering of a nearly free two-dimensional electron gas (2DEG) through surface defects, vacancies, step edges, or impurities leads to quantum interference patterns, which can directly be visualized in real space by scanning tunneling microscopy (STM) [2–5]. Such interference phenomena originate from the superposition of coherently scattered waves, which results in a spatial modulation of the surface electron local density of states (LDOS). Recently, such LDOS oscillations have been intensively utilized in energy-resolved differential conductance measurements with the scanning tunneling microscope (STM), so-called quasiparticle interference (QPI) mapping. This QPI mapping has the advantage that by Fourier transformation it permits access to the wave vector, i.e., k sensitivity, to the otherwise k -averaging scanning tunneling spectroscopy technique.

In particular, these waves have been reported for sp -derived Shockley-type surface states (sp -SS), which are found on various face-center cubic (fcc) noble metal (111) surfaces, including Cu, Ag, and Au [6–8]. In these materials delocalized sp -SS electrons are confined to the surface by the vacuum barrier on one side and a projected bulk L gap on the other side. The resulting electronic structure can be regarded as a model system for a quasi-two-dimensional electron gas (2DEG) that leads to characteristic surface properties, which have been investigated in numerous studies [9–12].

Owing to the electron's spin degree of freedom, the exchange energy in ferromagnetic materials results in an exchange splitting ΔE_{ex} of the electronic structure into majority (spin-up) and minority (spin-down) bands. Since the exchange splitting also affects Shockley-type surface states, in addition to the above-mentioned modulation of the LDOS, a spatial variation of the spin polarization could also be observed in several publications [13–15]. To the best of our

knowledge, however, the direct observation of the 2DEG dispersion relation of exchange-split Shockley-type sp -SS through an energy-dependent investigation of QPI maps has only been reported for the (111) surface of the 3d transition metal nickel (Ni) [16,17].

Surprisingly, these experimental QPI results are quite contradictory [16,17] and do not agree well with earlier results obtained theoretically by density functional theory (DFT) [18–20] or experimentally by photoemission spectroscopy (PES) [19,21,22] or inverse PES (IPES) [23–25]. Summarizing the available DFT and (I)PES data [16–25] it seems to be consensus that the electronic structure of Ni(111) around the Fermi level is dominated by an exchange-split Shockley-type sp -SS and a minority d -derived surface resonance (d -SR). But even though the qualitative band dispersion is unanimously agreed on, the exact parameters of the respective band onsets, effective masses, and the exchange splitting of the sp -SS have been discussed controversially. In the QPI study by Braun *et al.* [16] two isotropic wave vectors forming two rings in the Fourier-transformed QPI patterns are reported for the partially occupied, upwards dispersing sp -SS (also called S_1), which are ascribed to an exchange splitting $\Delta E_{\text{ex}} = 60 \pm 15$ meV between the majority and the minority part of sp -SS, $S_{1,\text{maj}}$ and $S_{1,\text{min}}$, respectively. However, this observation was only made after the deposition of Au atoms onto the Ni(111) surface, but not on pristine Ni(111) surface or close to step edges, as they reportedly result in stronger scattering than intrinsic defects.

These findings strikingly disagree with STM/STs and angle-resolved PES (ARPES) measurements by Nishimura *et al.* [17]. While Nishimura *et al.* only find a single circularly shaped contour in Fourier-transformed (FT) QPI patterns observed surface defects on Ni(111), they claim to be able to determine the exchange splitting to $\Delta E_{\text{ex}} \approx 190$ meV for the sp -SS by fitting a steplike feature in their STs data. In other words, their results suggest that only the majority spin component of sp -SS is observed by QPI and that the minority part is pushed far above E_F by the exchange interaction. However, they observe an extremely steep band dispersion (within the error bar same k value for all bias voltages), which

*pin-jui.hsu@physik.uni-wuerzburg.de

would result in an unrealistically small effective electron mass that is completely inconsistent with earlier PES and IPES data.

In this paper, we present a detailed QPI investigation of the Ni(111) surface. By analyzing Fourier-transformed (FT) QPI maps obtained over a wide range of bias voltages, not only the dispersion of the partially occupied, upwards dispersing Shockley-type sp -SS, but also of an occupied, downwards dispersing d -like surface resonance (d -SR) could be resolved. Interestingly, the FT-QPI maps of the sp -SS exhibit characteristic double ringlike features, which are interpreted as the majority and minority part of the exchange-split band. The exchange splitting is determined to $\Delta E_{\text{ex}} = 100 \pm 8$ meV. Quantum confinement phenomena in surface vacancy islands are employed to highlight and identify resonance peaks of the sp -SS by high-energy resolution STS spectra. Peak positions are analyzed within a one-dimensional (1D) quantum well model.

II. EXPERIMENTAL SETUP AND PROCEDURES

The experiments were performed in an ultrahigh vacuum (UHV) chamber with the base pressure of $p \leq 5 \times 10^{-11}$ mbar. The clean Ni(111) surface was prepared by cycles of Ar^+ ion sputtering with an ion energy of 500 eV and subsequent annealing up to 1000 K for several minutes. The cleanliness and undistorted face-center-cubic (fcc) crystalline structure were confirmed by Auger-electron spectroscopy (AES) and low-energy electron diffraction (LEED) [26], respectively. Vacancy islands were prepared by sputtering the clean surface at an ion current of $1 \mu\text{A}$ for a few seconds followed by 4 min postannealing up to 400 K. After preparation, the sample was immediately transferred into a home-built LT-STM (operation temperature $T = 5.5$ K). For so-called topography images the LT-STM was operated in the constant-current mode with a bias voltage (V_b) applied to the sample. For scanning tunneling spectroscopy (STS) measurements a small bias voltage modulation was added to U (frequency $\nu = 5.777$ kHz; amplitude 5 to 15 mV), such that tunneling differential conductance dI/dU spectra as well as dI/dU maps can be acquired by detecting the first harmonic signal with a lock-in amplifier.

III. RESULTS AND DISCUSSION

A typical large-scale STM topography of the clean Ni(111) surface is shown in Fig. 1(a). Four atomically flat surface terraces with a width of at least 100 nm can be seen which are separated by monatomic step edges. Within the field of view three protruding lines which occasionally cross step edges can be recognized [arrows in Fig. 1(a)]. We speculate that these features are caused by dislocations, which are probably pinned by defects inside the bulk. The inset of Fig. 1(a) displays a zoomed-in image obtained within the hatched box on top of an atomically flat terrace without any dislocations. Within the defect-free region marked by a blue dot in Fig. 1(a) we have confirmed the cleanliness by acquiring atomic resolution images [26]. Similar areas have been chosen for acquiring differential conductance dI/dU maps which will be presented further below.

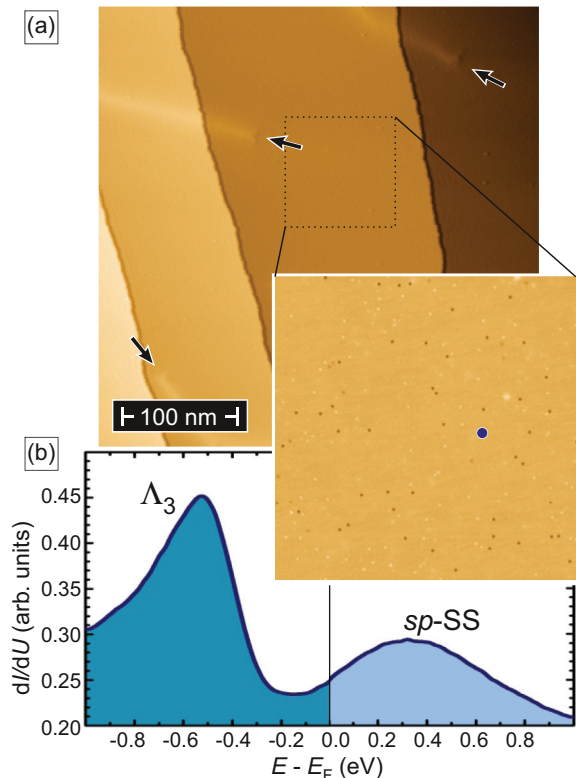


FIG. 1. (Color online) (a) The STM topography of clean Ni(111) (scan parameters: $U = +1.0$ V, $I = 300$ pA). Within the field of view the surface exhibits four atomically flat terraces, which are separated by three monatomic step edges. The three weakly protruding lines (arrows) are presumably caused by subsurface dislocations. Typically, QPI maps were obtained on large atomically flat surface areas, such as shown in the zoomed-in image in the inset. Constant-separation tunneling spectra were taken at defect-free regions, as marked by a solid blue dot in the inset of (a). (b) Typical tunneling spectrum of Ni(111); two broad maxima representing the Λ_3 bulk state and the Shockley-type sp -SS can be recognized (STS set-point parameters: $U = +1.0$ V; $I = 3.0$ nA).

A characteristic tunneling spectrum of Ni(111) is shown in the Fig. 1(b). It exhibits two broad maxima peaked at about -530 meV below and $+300$ meV above the Fermi level E_F , i.e., in the occupied and unoccupied states, respectively. This spectrum is in good agreement with previous observations published in Refs. [16,20], but differs significantly from the results of Pons *et al.* [12]. While Braun and Rieder [16] discuss the peaks as Ni 3d bands with purely minority spin character above but mixed spin below E_F , Dzemiantsova *et al.* [20] interpreted them as a minority spin surface resonance below and Shockley surface state with both spin characters above E_F based on density functional theory (DFT) calculations. The latter interpretation is also consistent with ARPES measurements, where the Λ_3 bulk state is responsible for the maximum in the occupied states while another maximum in the unoccupied states most likely originates from a Shockley-type surface state sp -SS, which is partially occupied with the band onset close to the E_F [19,21,22]. The peaks are labeled accordingly in Fig. 1(b).

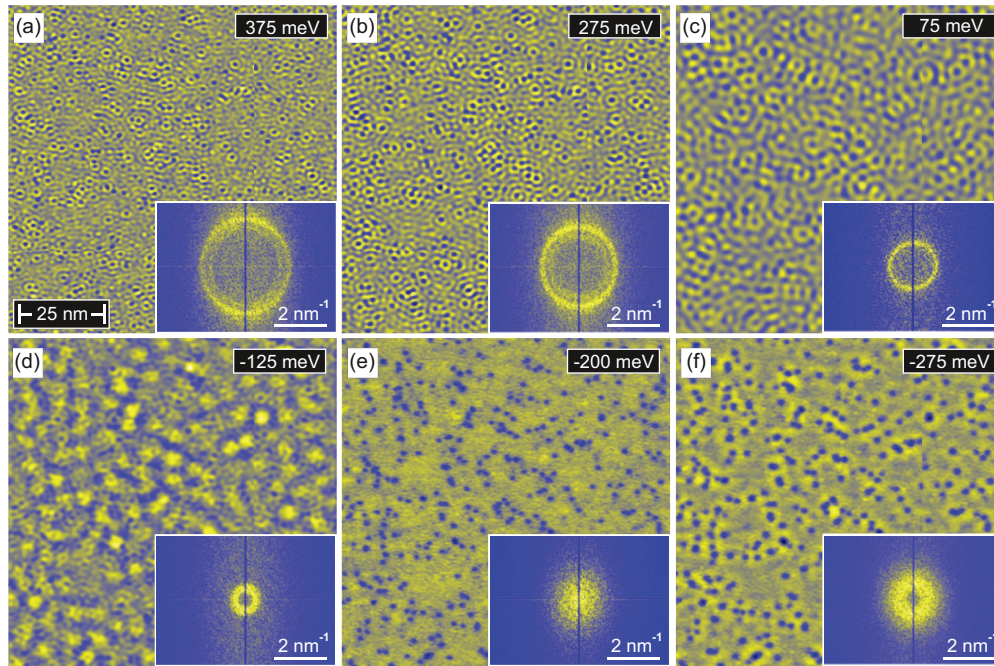


FIG. 2. (Color online) (a)–(f) QPI maps taken at energies indicated in the upper right and their respective FT (insets). Obviously, the real space QPI scattering wavelength continuously increases (corresponding to the reduction of the reciprocal scattering vector in the insets) as the energy is lowered from +375 meV (a) down to -125 meV (d). Note that the FT-QPI maps in (a) and (b) reveal two scattering wave vectors, as indicated by double-ring features in the reciprocal space. This double ring cannot only be resolved on flat terraces, but also close to step edges of the pristine Ni(111) surface. No particular pattern is detected at -200 meV (e). Below -275 meV another pattern with a specific wavelength and a related ring in the FT appears in (f). All the QPI maps were taken at the constant tunneling resistance of 0.1 G Ω .

It is a severe limitation of simple constant-separation tunneling spectroscopy measurements that details of the surface electronic structures, such as the energy band dispersions, exact band onsets, or effective electron masses cannot be obtained. In order to overcome this limitation we have taken differential conductance dI/dU maps with the bias voltage range -500 meV $\leq U \leq +500$ meV. This technique, for which the term quasiparticle interference (QPI) mapping has been coined, images the standing electron waves of surface electronic states that result from coherent backscattering at impurities or other defects. Since electrons that reside in a specific state possess a unique energy–wavelength relation, the dispersion in reciprocal k space can be obtained through Fourier-transformed (FT) QPI maps.

Figures 2(a)–2(f) presents a series of energy-dependent QPI maps taken between $E - E_F = +375$ meV (empty states) and -275 meV (occupied states). The respective Fourier-transformed (FT) images are shown in the insets. At this point we would like to emphasize that—in contrast to earlier experiments where a scattering pattern on flat terraces could only be seen upon the deposition of Au atoms [16]—our data were obtained on the pristine Ni(111) surface. In this case the interference of coherent electronic states is caused by reflection at the much weaker scattering potentials of the few remaining impurities present on the surface. The nature of these defects is unknown and their concentration amounts to about 0.3% of surface atoms only. Thereby we are able to avoid any potential Au- or adsorbates-induced modifications of the Ni(111) surface electronic structures, which is chronically

susceptible even to minute amounts of surface contaminants [16,19,23].

Close inspection of the FT-QPI patterns (insets) in the unoccupied energy range between +250 and +500 meV reveals double-ring-like features, i.e., the coexistence of two wave vectors, which are both isotropic (as indicated by their circular shape) but exhibit different length (radius of the circle). Both, the inner and outer rings show a clear dispersion of the wave vector with energy [cf. Figs. 2(a) and 2(b)]. We also denote that—in contrast to Ref. [16]—the presence of double-ring-like feature cannot only be observed on large, atomically flat terraces but also close to step edge [26]. In fact, within our measurement accuracy the electronic properties in the middle of a terrace, i.e., at a distance >50 nm from a step edge, are identical to those measured in close proximity (≈ 10 nm) to the step edge. Since the experiments presented here were performed on clean Ni(111) and since our results are, as we will describe below, largely consistent with earlier ARPES and IPES measurements, we believe that our observations are more intimate related to the intrinsic properties on Ni(111) surface, whereas the results of Ref. [16] are probably representative for Au-covered Ni(111).

As we move to the energy range between $+75$ and -125 meV, the signal responsible for the inner ring of the FT-QPI pattern vanishes and only the outer ring remains detectable while continuously reducing the reciprocal lattice vector, corresponding to an increasing wavelength in the real-space dI/dU maps. Eventually, this ringlike feature also disappears as the energy is lowered below about -150 meV.

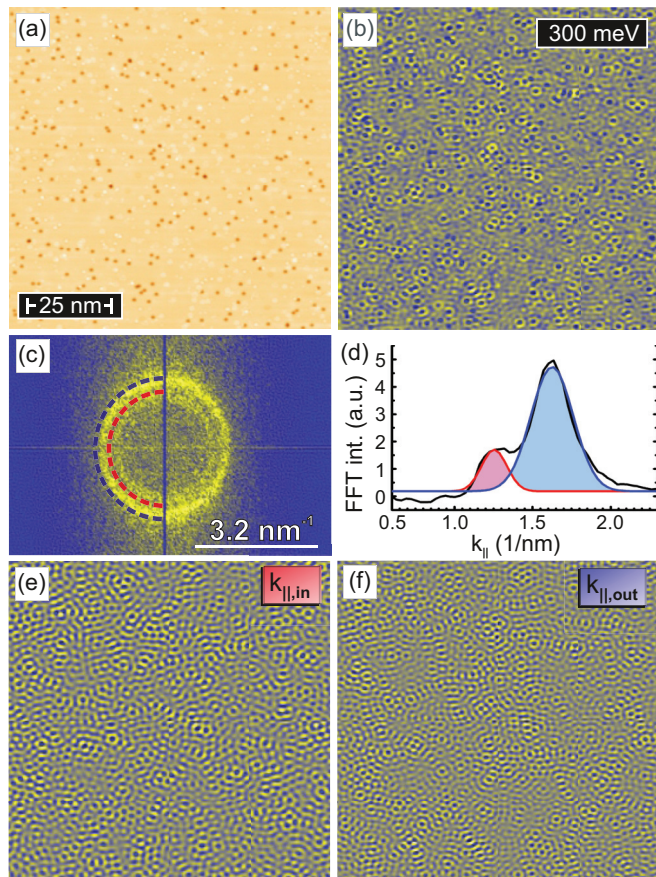


FIG. 3. (Color online) (a) Constant-current topograph of Ni(111) and (b) the simultaneously recorded QPI map at 300 meV (tunneling resistance: 0.1 G Ω). The corresponding FT-QPI pattern is shown in (c). The radial average of the double-ring feature is displayed in (d). The data can nicely be fitted with two Gaussian peaks. Inverse FT-QPI patterns within a narrow range of frequencies around the inner red and the outer blue circle, $k_{||,in}$ and $k_{||,out}$, are presented in (e) and (f), respectively.

No specific wavelength is detected between about -150 and -240 meV. Surprisingly, another feature the wave vector of which rapidly increases appears at even lower energy.

The ringlike shape of FT-QPI patterns in Fig. 2 indicates that the dispersion relations of the electronic states detected here are highly isotropic within the surface plane. Therefore, a better signal-to-noise ratio can be obtained by analyzing the radial average of the ringlike feature at different energies. This is illustrated in Fig. 3, which shows a constant-current topograph [Fig. 3(a)] of the clean Ni(111) surface taken at $+300$ meV and the simultaneously recorded dI/dU or QPI map [Fig. 3(b)]. The FT-QPI map is presented in Fig. 3(c). The double-ring feature mentioned above has been emphasized by red and blue semicircles. The corresponding radially averaged line profile is displayed in Fig. 3(d). For quantitative analysis the two peaks were fitted with two Gaussians, whereby the peak position and the full width at half maximum (FWHM) have been independently optimized. In order to exclude that the two peaks are caused by noise or other artifacts, the inverse FT-QPI pattern within a narrow range of frequencies around the inner red and the outer blue circle, $k_{||,in}$ and $k_{||,out}$,

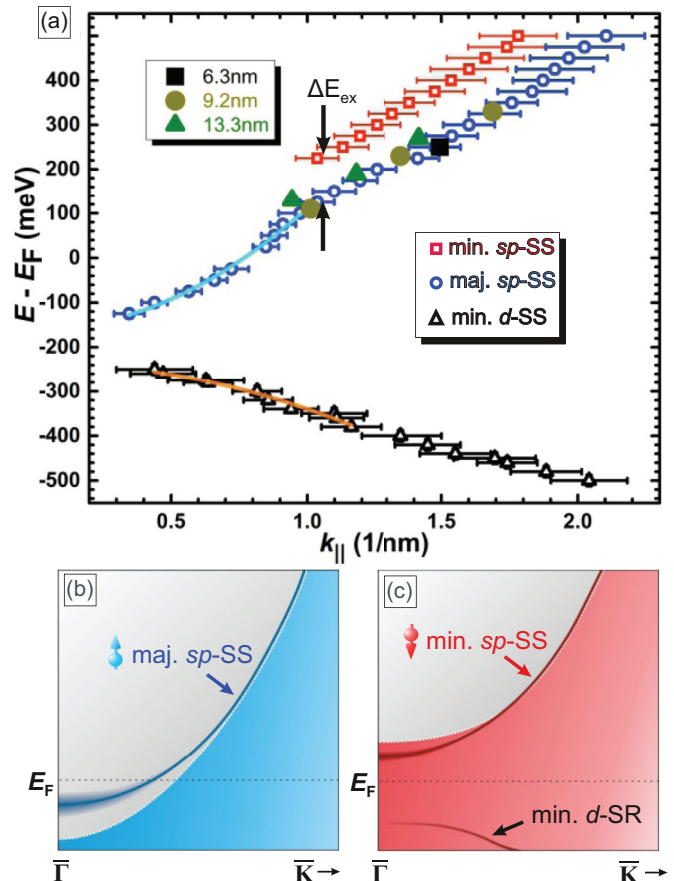


FIG. 4. (Color online) (a) Energy dispersion relation extracted from FT-QPI patterns. The two electronlike upward dispersing bands, which correspond to the double-ring FT-QPI features discussed in detail in Fig. 3, are interpreted as an sp -like Shockley surface state, sp -SS. This surface state is exchange split into a minority (red) and a majority (blue) spin part. The exchange splitting amounts to $\Delta E_{ex} = (100 \pm 8)$ meV (black arrows). For the majority part, a parabolic dispersion (light blue line) persists up to $+100$ meV. The holelike downward dispersion (black triangles) corresponds to a d -like surface resonance (d -SR). The fit (orange line) gives a band onset and the effective mass of (-235 ± 5) meV and $m^* = (-0.36 \pm 0.05)m_e$, respectively. Schematics of the majority and minority bands are shown in (b) and (c), respectively (see text for details).

are presented in Figs. 3(e) and 3(f), respectively. Indeed, the spatial distribution of both signals closely correspond to the topography of Fig. 3(a), thereby confirming the existence of two distinct coherent electronic features in the band structure of Ni(111).

Figure 4(a) summarizes the results of the QPI maps we have taken within the energy range of ± 500 meV around the Fermi level. This dispersion relations was obtained by fitting radially averaged profiles of FT-QPI maps, such as the one shown in Fig. 3(d), with up to two Gaussian functions (also see Fig. S4 for further data). The horizontal error bars correspond to the FWHM width of the fitted peaks. Three dispersing branches can clearly be recognized in Fig. 4(a). First, we take a close look at the two electronlike upward dispersing bands, which correspond to the double-ring FT-QPI features discussed in detail in Fig. 3. Although their dispersion extends far into

the unoccupied energy region the band onset of the lower band (blue open circles) is energetically located below the Fermi level. Since the curvature of this lower electronlike band significantly changes at about +100 meV we have limited the fitting procedure to the energy range below that threshold. A parabolic fit results in a band onset at (-160 ± 5) meV and an effective mass $m^* = (+0.14 \pm 0.04)m_e$.

These parameters are in almost perfect agreement with earlier experimental [21,25] and theoretical data [18,25] of the majority part of sp -SS [18,21,25]. Consistently, the second dispersion with slightly smaller k values observed above electron energies above +250 meV can be attributed to the minority part of sp -SS [23–25]. The corresponding strength of magnetic exchange splitting can be extrapolated to a value of $\Delta E_{\text{ex}} = 100 \pm 8$ meV, which is in a better agreement with IPES results ($\Delta E_{\text{ex}} \approx 100$ meV) [23] than the earlier claim made on the basis of STS spectra measurements [17]. Based on a parabolic fit of the downward dispersing band (black open triangles), which can be found below the Fermi level in Fig. 4(a), the band onset has been determined to (-235 ± 5) meV and the effective mass $m^* = (-0.36 \pm 0.05)m_e$. These parameters of the downward dispersing band are in excellent agreement with a surface resonance (d -SR) reported by Kutzner *et al.* [21].

In this context we would like to briefly discuss our observation that parabolic fitting procedures result in an excellent agreement for relatively small k values, i.e., experimental data close to the $\bar{\Gamma}$ point, but significantly differ as we move further away from the center of the surface Brillouin zone. We attribute this observation to the previously reported considerable hybridization between surface states or resonances and d -like bulk bands [21,23,25]. Recently, similar deviations from a simple parabolic dispersion expected for a quasifree 2DEG have been reported not only the noble, but also for transition metal surfaces [27,28].

Based on a comparison with earlier theoretical predictions and experimental results, Figs. 4(b) and 4(c) summarize our results in the energy range around E_F within schematic majority and minority band structures showing details of dispersion relations [18,19,25]. We note that the electrons of the sp -like Shockley surface state, sp -SS, presumably have the same effective mass for majority and minority spins, thereby producing the same curvature in energy dispersion relations. Close to the $\bar{\Gamma}$ point of the surface Brillouin zone the majority part of this surface state is located well inside the projected bulk band gap [see Fig. 4(b)]. Accordingly, the QPI map is dominated by the scattering of quasifree majority surface electrons in this energy regime and both the band onset as well as the effective electron mass obtained from fitting the dispersion relation are in good agreement with earlier photoemission results [21]. As we move to higher energies above about +100 meV a change of curvature can be recognized which we interpret as a result of hybridization with bulk states. Qualitatively, a similar picture has been described in an early spin-resolved inverse photoemission study (see Fig. 4 in Ref. [25]) and in a combined STS with multiphoton photoemission study [28]. In the latter it was observed that the surface state is bending towards the edge of the projected bulk bands as soon as their separation in k (at a certain E) is getting too small.

As can be seen in the Fig. 4(a), the situation is markedly different for the minority part of sp -SS. In this case we cannot detect the onset of the band, i.e., the long wavelength part of the QPI pattern. Only above about +220 meV the band dispersion can clearly be resolved [see red squares in Fig. 4(a)]. As schematically represented in Fig. 4(c), we interpret the absence of a QPI pattern as a consequence of the strong hybridization with bulk states close to $\bar{\Gamma}$. Obviously, the minority part of sp -SS is well inside the gap of the projected bulk band structure only for relatively large k values, but merges into bulk electronic states close to the band onset. Moreover, we are able to detect a d -derived surface resonance (d -SR) which exhibits a holelike downward dispersion in Fig. 4(a). Both the band onset and the effective mass of this occupied d -SR are consistent with previous studies as mentioned in the above paragraph [25,32]. These earlier studies also reveal a strong hybridization of this surface electronic feature with d -like bulk states, clearly distinguishing it from a surface state which is located within a projected bulk band gap.

So far we are left with the situation that the information obtained from constant-separation tunneling spectroscopy on one hand and through Fourier-transformed quasiparticle interference mapping on the other hand shows very little overlap. In order to investigate if signatures of the surface state and surface resonance bands described in Fig. 4 can also be detected in constant-separation STS, we have prepared vacancy islands with various sizes. A topographic image of those vacancy islands is shown in Fig. 5(a). As has been shown on several other surfaces [29–31], the quantum confinement of Shockley-like surface states into nanoscale environments, such as islands or holes, may leads to pronounced peaks in the tunneling spectra.

Indeed, comparison of the three topmost high-energy-resolution tunneling spectra of Fig. 5(b), which have been taken with the tip positioned above the center of the three vacancy islands marked by correspondingly colored dots in the inset of Fig. 5(a), with the spectrum of the Ni(111) surface [bottom of Fig. 5(b)] reveals the appearance of additional peaks at characteristic quantization energies (see arrows). These peaks can be interpreted within a 1D quantum well model by the resonant formation of standing waves within the confinement potential of the vacancy islands. We have verified that an excellent agreement within the error bar of our experimental data is also achieved for states that exhibit the so-called A_1 symmetry within an existing two-dimensional (2D) model [7]. Since the 1D approach allows an easier intuitive understanding we will restrict the following discussion to this model.

As schematically shown in Fig. 5(c) an STS peak is expected whenever the electron wave lengths λ matches the diameter of a vacancy island D and the density of states peaks at the tip position, i.e., the vacancy island center, or, in other words, if $D/\lambda_n = (n + 1)/2$, with $n = 0, 2, 4, 6 \dots$. In contrast, odd numbers of n would result in a node of the wave function in the island center and are therefore not expected to result in a resonant enhancement of the spectroscopic dI/dU signal. As an example Fig. 5(d) shows the topography (top panel) and dI/dU maps taken at three outstanding bias voltages (indicated on the right of the bottom three panels) of the vacancy island with an effective lateral boundary length of

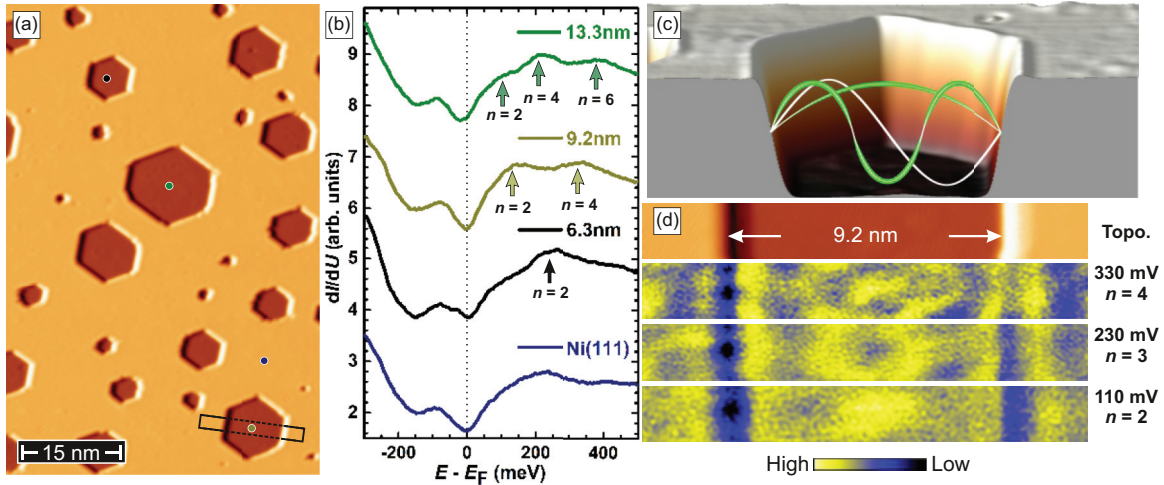


FIG. 5. (Color online) (a) Topographic STM image of a Ni(111) surface, which has been Ar^+ bombarded and annealed to intentionally create vacancy islands (scan parameters: $U = +1.0$ V, $I = 300$ pA). (b) STS spectra taken at the center of vacancy islands with different sizes and on the flat Ni(111) surface, as marked by differently colored solid dots in (a) (STS set-point parameters: $U = -0.3$ V, $I = 1.0$ nA). The arrows in (b) indicate peaks that originate from energy levels due to quantum confinement of the unoccupied sp -SS. The wavelengths of the resonances can be estimated on the basis of a simple quantum-mechanical model as illustrated in (c) with $\lambda_n = (n + 1)/2$, where $n = 0, 2, 4, 6, \dots$. The analysis of $k_n(E_n)$ with size dependence have been arranged into the Fig. 4(a) together with the dispersion relations, i.e., colored triangular, circular, and square dots. (d) Topography (top panel) and differential conductance dI/dU maps (bottom three panels) taken at the 9.2 nm vacancy within the area indicated by a black rectangle in (a) at bias voltages that correspond to quantum states with $n = 2, 3$, and 4, respectively. Only those states with an antinode of the dI/dU signal in the center of the vacancy island, i.e., with even n , show up as peaks in the respective spectra shown in (b).

9.2 nm. While the states with $n = 2$ ($U = 110$ mV) and $n = 4$ ($U = 330$ mV) exhibit clear maxima in the island center, the wave function of the state with $n = 3$ ($U = 230$ mV) leads to a minimum of the density of states.

Based on the relation $k_n = 2\pi/\lambda_n$ the quantized wave vectors k_n can be extracted. These $k_n(E_n)$ values have been arranged into the dispersion relation of Fig. 4(a). Please note that the values obtained from three vacancy holes of Figs. 5(a) and 5(b) are shown as correspondingly colored triangular ($D = 13.3$ nm), circular ($D = 9.2$ nm) and square ($D = 6.3$ nm) dots. They agree well with the band dispersion of sp -SS. This directly indicates that the main contributions to quantum confinement phenomena of surface electrons originate from the unoccupied part of the Shockley-type sp -SS.

IV. SUMMARY

In conclusion, we have carried out a systematic quasiparticle interference (QPI) study of energy dispersion relations of surface electronic states on pristine Ni(111) surface. Our data show two states, an upward dispersing Shockley-type sp -SS

with an effective electron mass $m^* = (+0.14 \pm 0.04)m_e$ and a downward dispersing d -SR with $m^* = (-0.36 \pm 0.05)m_e$. The data also reveal that the sp -SS is exchange-split into a majority and a minority spin part, as indicated by the appearance of two intraband scattering features in Fourier-transformed QPI maps. We find a significant deviation from parabolic band dispersion at energies far away from the onset of the respective band onsets. This is interpreted as a result of hybridization between surface and bulk states. Based on a comparison of these effects in minority and majority bands we obtain a better understanding of spin-resolved surface electronic structures close to E_F . We employ vacancy islands with different diameters to examine quantum confinement phenomena of the sp -SS by high-resolution STS spectra. We find that the quantization of wave vectors $k_n(E_n)$ can be understood within a 1D quantum well model, which agrees well with the dispersion relations of the unoccupied part of the sp -SS.

ACKNOWLEDGMENT

This work has been funded by Deutsche Forschungsgemeinschaft (Grant No. BO1468/22-1).

- [1] C. Davisson and L. H. Germer, *Nature (London)* **119**, 558 (1927).
 [2] M. F. Crommie, C. P. Lutz, and D. M. Eigler, *Nature (London)* **363**, 524 (1993).

- [3] E. J. Heller, M. F. Crommie, C. P. Lutz, and D. M. Eigler, *Nature (London)* **369**, 464 (1994).
 [4] Y. Hasegawa, and Ph. Avouris, *Phys. Rev. Lett.* **71**, 1071 (1993).

- [5] L. Bürgi, O. Jeandupeux, A. Hirstein, H. Brune, and K. Kern, *Phys. Rev. Lett.* **81**, 5370 (1998).
- [6] G. Hörmandinger, *Phys. Rev. B* **49**, 13897 (1994).
- [7] J. Li, W.-D. Schneider, S. Crampin, and R. Berndt, *Sur. Sci.* **422**, 95 (1999).
- [8] W. Chen, V. Madhavan, T. Jamneala, and M. F. Crommie, *Phys. Rev. Lett.* **80**, 1469 (1998).
- [9] M. G. Vergniory, J. M. Pitarke, and P. M. Echenique, *Phys. Rev. B* **76**, 245416 (2007).
- [10] K. Pohl, B. Diaconescu, G. Vercelli, L. Vattuone, V. M. Silkin, E. M. Chulkov, P. M. Echenique, and M. Rocca, *Europhys. Lett.* **90**, 57006 (2010).
- [11] S. LaShell, B. A. McDougall, and E. Jensen, *Phys. Rev. Lett.* **77**, 3419 (1996).
- [12] S. Pons, P. Mallet, L. Magaud, and J. Y. Veuillein, *Europhys. Lett.* **61**, 375 (2003).
- [13] K. von Bergmann, M. Bode, A. Kubetzka, M. Heide, S. Blügel, and R. Wiesendanger, *Phys. Rev. Lett.* **92**, 046801 (2004).
- [14] L. Niebergall, V. S. Stepanyuk, J. Berakdar, and P. Bruno, *Phys. Rev. Lett.* **96**, 127204 (2006).
- [15] H. Oka, P. A. Ignatiev, S. Wedekind, G. Rodary, L. Niebergall, V. S. Stepanyuk, D. Snader, and J. Kirschner, *Science* **327**, 843 (2010).
- [16] K. F. Braun and K. H. Rieder, *Phys. Rev. B* **77**, 245429 (2008).
- [17] Y. Nishimura, M. Kakeya, M. Higashiguchi, A. Kimura, M. Taniguchi, H. Narita, Y. Cui, M. Nakatake, K. Shimada, and H. Namatame, *Phys. Rev. B* **79**, 245402 (2009).
- [18] T. Ohwaki, D. Wortmann, H. Ishida, S. Blügel, and K. Terakura, *Phys. Rev. B* **73**, 235424 (2006).
- [19] J. Lobo-Checa, T. Okuda, M. Hengsberger, L. Patthey, T. Greber, P. Blaha, and J. Osterwalder, *Phys. Rev. B* **77**, 075415 (2008).
- [20] L. V. Dzemiantsova, M. Karolak, F. Lofink, A. Kubetzka, B. Sachs, K. von Bergmann, S. Hankemeier, T. O. Wehling, R. Frömter, H. P. Oepen, A. I. Lichtenstein, and R. Wiesendanger, *Phys. Rev. B* **84**, 205431 (2011).
- [21] J. Kutzner, R. Paucksch, C. Jabs, H. Zacharias, and J. Braun, *Phys. Rev. B* **56**, 16003 (1997).
- [22] T. Okuda, J. Lobo-Checa, W. Auwärter, M. Morscher, M. Hoesch, V. N. Petrov, M. Hengsberger, A. Tamai, A. Dolocan, C. Cirelli, M. Corso, M. Muntwiler, M. Klöckner, M. Roos, J. Osterwalder, and T. Greber, *Phys. Rev. B* **80**, 180404 (2009).
- [23] M. Donath, F. Passek, and V. Dose, *Phys. Rev. Lett.* **70**, 2802 (1993).
- [24] M. Donath, *Surf. Sci. Rep.* **20**, 251 (1994).
- [25] J. Braun and M. Donath, *J. Phys.: Condens. Matter.* **16**, S2539 (2004).
- [26] See Supplemental Material at <http://link.aps.org/supplemental/10.1103/PhysRevB.89.155413> for details of atomic resolution data, QPI scattering at step edges, as well as amplitudes and bias dependence of radial-averaged profiles.
- [27] J. Wiebe, F. Meier, K. Hashimoto, G. Bihlmayer, S. Blügel, P. Ferriani, S. Heinze, and R. Wiesendanger, *Phys. Rev. B* **72**, 193406 (2005).
- [28] A. A. Ünal, C. Tusche, S. Ouazi, S. Wedekind, C. T. Chiang, A. Winkelmann, D. Sander, J. Henk, and J. Kirschner, *Phys. Rev. B* **84**, 073107 (2011).
- [29] M. F. Crommie, C. P. Lutz, and D. M. Eigler, *Science* **262**, 218 (1993).
- [30] J. Li, W. D. Schneider, R. Berndt, and S. Crampin, *Phys. Rev. Lett.* **80**, 3332 (1998).
- [31] L. Niebergall, G. Rodary, H. F. Ding, D. Sander, V. S. Stepanyuk, P. Bruno, and J. Kirschner, *Phys. Rev. B* **74**, 195436 (2006).
- [32] J. Braun and M. Donath, *Europhys. Lett.* **59**, 592 (2002).